

# Gamma-rays from a $^{241}\text{AmO}_2$ source in an $\text{Al}_2\text{O}_3$ matrix

Antonín Krása and Arjan Plompen



EUR 24818 EN - 2011

The mission of the JRC-IRMM is to promote a common and reliable European measurement system in support of EU policies.

European Commission  
Joint Research Centre  
Institute for Reference Materials and Measurements

#### Contact information

Address: Retieseweg 111, 2440 Geel, Belgium

E-mail: [Arjan.Plompen@ec.europa.eu](mailto:Arjan.Plompen@ec.europa.eu)

Tel.: +32 (0) 45 71 381

Fax: +32 (0) 45 71 381

<http://irmm.jrc.ec.europa.eu/>

<http://www.jrc.ec.europa.eu/>

#### Legal Notice

Neither the European Commission nor any person acting on behalf of the Commission is responsible for the use which might be made of this publication.

***Europe Direct is a service to help you find answers  
to your questions about the European Union***

**Freephone number (\*):**

**00 800 6 7 8 9 10 11**

(\*) Certain mobile telephone operators do not allow access to 00 800 numbers or these calls may be billed.

A great deal of additional information on the European Union is available on the Internet.  
It can be accessed through the Europa server <http://europa.eu/>

JRC 64615

EUR 24818 EN

QÓPÁÍ Ì ÈÇÈ JÈÇÈ Í È Á; Ì ÈÇÈ JÈÇÈ Í ÈÇÈ Á-Á

ISSN FÈÍ È Í JHÇ; Ì ÈÇÈ 831-9424 Ç Á-Á

doi:10.2787/43859

Á

Luxembourg: Publications Office of the European Union

© European Union, 2011

Á

Reproduction is authorised provided the source is acknowledged

*Printed in Belgium*

## **Gamma-rays from a $^{241}\text{AmO}_2$ source in an $\text{Al}_2\text{O}_3$ matrix**

## Introduction and summary

Americium is a minor actinide making an important component of high level nuclear waste. A considerable number of studies have been performed or are ongoing to determine cross sections for neutron-induced reactions on  $^{241}\text{Am}$ . Recently, two measurements of the neutron-induced capture reaction on  $^{241}\text{Am}$  were performed at the n\_TOF facility of CERN. One of these measurements used the  $\text{C}_6\text{D}_6$  detectors, the other used the  $\text{BaF}_2$  calorimeter. In both cases, a sample from IRMM was used that had been prepared at ITU [1]. This sample consisted of  $^{241}\text{AmO}_2$  which was dispersed in a matrix of  $\text{Al}_2\text{O}_3$ . The material was pressed into a disk, calcined and enclosed in an aluminium container. It contained about 40 mg of  $^{241}\text{Am}$ . The samples had been prepared for measurements of the  $^{241}\text{Am}(n,2n)^{240}\text{Am}$  reaction cross section [2]. Further details about the sample and these measurements may be found in [1,2].

During the measurements at CERN it was noted that several high energy  $\gamma$ -rays were emitted by the sample. This presented the question as to the exact energies and origin of these  $\gamma$ -rays. For this purpose the sample was returned to IRMM and  $\gamma$ -ray spectroscopy with a high purity germanium (HPGe) detector was performed. The energy and origin of most  $\gamma$ -rays was determined in this way. Here we report about these measurements paying attention only to  $\gamma$ -rays that are not known from the decay of  $^{241}\text{Am}$  [3] and to the  $\gamma$ -ray energy range from 844 keV to 13 MeV.

There are two mechanisms leading to gamma-ray emission. First there is the natural activity of  $^{241}\text{Am}$  and the three known actinide impurities:  $^{237}\text{Np}$  (0.021),  $^{233-236,238}\text{U}$  (0.000094) and  $^{239,240}\text{Pu}$  (0.0017; fractions by weight). Of these  $^{241}\text{Am}$  dominates the spectrum, even after applying absorbers to completely stop the 59 keV transition. From the main impurity,  $^{237}\text{Np}$ , no gammas are found but there are those of its daughter,  $^{233}\text{Pa}$ . For the other actinide impurities and their descendants no gamma-rays were found in the measurement. The second source of gamma-rays are alpha-induced reactions. For energies below the maximum alpha energy of 5.485 MeV, Q-values, thresholds and main characteristic gamma-rays are given in table 1 for the likely candidate reactions. Reactions conclusively identified are  $^{27}\text{Al}(\alpha,\alpha'\gamma)^{27}\text{Al}$ , and  $^{27}\text{Al}(\alpha,p)^{30}\text{Si}$  and these explain nearly everything besides the  $^{241}\text{Am}$  and  $^{233}\text{Pa}$  gammas already discussed. There is a clear indication for the  $^{27}\text{Al}(\alpha,n)^{30}\text{P}$  reaction, but for the  $^{27}\text{Al}(\alpha,\gamma)^{31}\text{P}$  reaction the evidence is not conclusive due to an overlap with gammas from  $^{30}\text{Si}$ . No evidence was found for  $\alpha$ -induced reactions on the isotopes of oxygen.

The measurements are described in the section Experiment. A table with  $\gamma$ -ray energies and figures with the  $\gamma$ -ray spectra are given in the section Results. The origin of these gammas is indicated there as well. Only three  $\gamma$ -rays remain unattributed.

A spectrum taken at CERN with a germanium detector showing many additional lines cannot be confirmed. Most likely this was taken under very poor background conditions.

**Table 1:** Q-values for alpha-induced reactions with thresholds below 6 MeV. Values are rounded to 1 keV. The gamma-ray energy for the transition from the first few excited states to the ground state are given, as well. The product nuclei are stable except for  $^{30}\text{P}$  which decays with a half life of 2.5 minutes to  $^{30}\text{Si}$ . All decay gamma-rays are very weak except for the 511 keV annihilation radiation from the  $^{30}\text{P}$  decay.

Reaction	Q-value (keV)	Threshold (keV)	Main gammas (keV)
$^{27}\text{Al}(\alpha, \gamma)^{31}\text{P}$	9669	0	1266
$^{27}\text{Al}(\alpha, p)^{30}\text{Si}$	2372	0	2235
$^{27}\text{Al}(\alpha, \gamma')^{27}\text{Al}$	-844	969	844
$^{27}\text{Al}(\alpha, n)^{30}\text{P}$	-2643	3035	677, 709, 1454
$^{16}\text{O}(\alpha, \gamma)^{20}\text{Ne}$	4730	0	1634
$^{17}\text{O}(\alpha, \gamma)^{21}\text{Ne}$	7348	0	351, 1395
$^{17}\text{O}(\alpha, n)^{20}\text{Ne}$	587	0	1634
$^{17}\text{O}(\alpha, \gamma')^{17}\text{O}$	-871	1076	871, 2184
$^{17}\text{O}(\alpha, n)^{16}\text{O}$	-4143	5119	6049
$^{18}\text{O}(\alpha, \gamma)^{22}\text{Ne}$	9668	0	1275
$^{18}\text{O}(\alpha, \gamma')^{18}\text{O}$	-1982	2423	1982
$^{18}\text{O}(\alpha, n)^{21}\text{Ne}$	-696	851	351, 1395

## Experiment

The americium sample was measured on a HPGe spectrometer (coaxial type with 94% relative efficiency). The sample was placed approximately 10 cm from the detector cap. Lead and copper filters (1 cm in thickness each) were placed between the sample and the detector in order to suppress low-energy  $\gamma$ -rays. Data acquisition was done using the IRMM's DAQ-2000 system.

The measurement was performed twice, each time covering a different energy region by varying the coarse gain of the spectroscopy amplifier:

- 1) 200-2700 keV – the gain was set to 50 (the measurement lasted 16 h),
- 2) 1100-13000 keV – the gain was set to 10 (the measurement lasted 23 h).

The energy calibration was done using a  $^{60}\text{Co}$  calibration standard (1173.2 keV and 1332.5 keV lines and their summing coincidence peak 2505.7 keV) and the annihilation peak at 511 keV. After the measurements, the energy calibration was refined with several peaks from the spectra of the americium sample, see **Fig. 1**. Results show that a linear fit works well also at the higher energies.

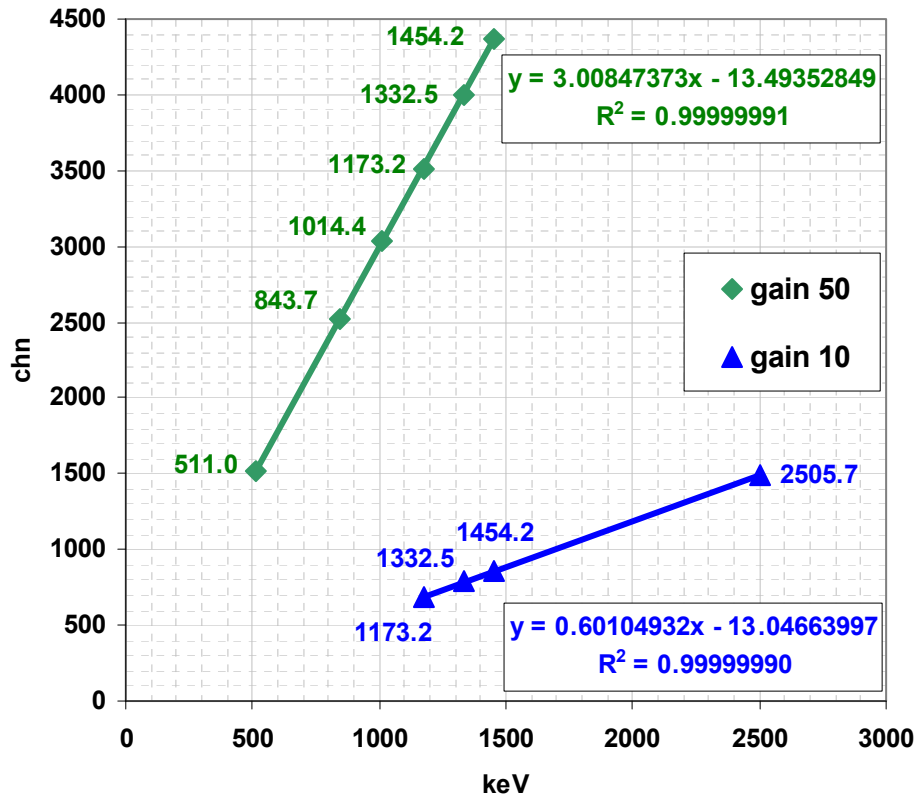


**Figure 1: The energy calibrations of the HPGe detector. The fits with a linear function are shown as well.**

## Results

The evaluated decay data for observed  $\gamma$ -rays coming from  $\alpha$ -interactions in aluminium are listed according in **Tables 2-5**. The  $\gamma$ -rays of  $^{233}\text{Pa}$ , the daughter of  $^{241}\text{Am}$  are listed in **Table 6**. The level and decay schemes highlighting the observed transitions are shown **Figures 2-5**.

**Table 7** summarizes the observed peaks, their structure, net peak areas and corresponding count rates for both measurements. Many of the observed peaks are very broad. This is due to overlap of gammas from different origin and/or to the Doppler effect which is significant for these light nuclei. The somewhat higher count rate for the 1454.2 keV line in the case of the measurement with the gain set to 10 could be caused by the contribution of 1460.8 keV of  $^{40}\text{K}$ , which was clearly separated in the case of the measurement with the gain set to 50.

The measured spectra in the whole energy range are shown in **Figure 6** for a gain of 50 and in **Figure 13** for a gain of 10. Detailed views for each spectrum are given in **Figures 7-12**, and **14-17**. Different colours are used to distinguish different reactions. In the high-energy region, which we paid attention to, the only strong  $\gamma$ -ray remaining unidentified is 4300 keV. Although a gamma-ray of 4302 keV is emitted by an excited state in  $^{30}\text{Si}$ , the picture is inconsistent since gammas emitted by the same level with similar or higher intensity are not observed (3039 keV overlaps with 3043 keV, 6537 and 2768 keV are not observed). There are five unidentified weak and narrow peaks at 7124, 7303, 7400, 7634, 7913 keV, see **Figure 17** and **Table 7**. It is likely that these are due to a capture reaction, but the target was not identified.

For comparison, the spectrum of the americium sample measured at CERN in December 2010 is shown in **Figure 18**. It covers the energy range from 1400 to 2650 keV. The line at 2235 keV ( $^{30}\text{Si}$ ) corresponds to what we observed, but other lines are redundant most likely as a result of a large background emphasizing for example the 2614.5 keV of  $^{208}\text{Tl}$ . Some lines that we clearly observe are not seen in this spectrum, most likely because they are weak and do not show on a linear scale after a short measurement.

**Table 2: Level and decay data for observed gammas from the  $^{27}\text{Al}(\alpha, \alpha'\gamma)^{27}\text{Al}$  reaction [4].**

$E_{\text{level}}$ [keV]	$E_{\gamma}$ [keV]	$I_{\gamma}$ [%]
843.76	843.74	100
1014.45	1014.42	100
2734.9	1720.3	100
2982.00	2981.82	100
3004.2	3004	100

**Table 3: Level and decay data for observed gammas from the  $^{27}\text{Al}(\alpha, p)^{30}\text{Si}$  reaction [5].**

$E_{\text{level}}$ [keV]	$E_{\gamma}$ [keV]	$I_{\gamma}$ [%]
2235.322	2235.23	100
3498.49	1263.13	100
	3498.33	98
3769.48	1534.12	100
	3769.22	85
3787.72	1552.36	100
4810.31	1311.8	89
	4810	100
4830.85	2595.39	100
5231.38	1732.7	100
5279.37	3043.2	100
5487.5	1989.02	96
	3252	100
5950.73	3714.9	100
6503.41	1271.9	100
6537.5	3039	100

**Table 4: Level and decay data for observed gammas from the  $(\alpha, n)^{30}\text{P}$  reaction [5].**

$E_{\text{level}}$ [keV]	$E_{\gamma}$ [keV]	$I_{\gamma}$ [%]
708.7	708.7	100
1454.23	1454.23	100
1973.27	1264.57	100

**Table 5: Level and decay data for observed gammas from the  $^{27}\text{Al}(\alpha, \gamma)^{31}\text{P}$  reaction [4].**

$E_{\text{level}}$ [keV]	$E_{\gamma}$ [keV]	$I_{\gamma}$ [%]
1266.15	1266.12	100
2233.7	2233.6	100

**Table 6: Decay data for observed gammas from  $^{233}\text{Pa}$  decay [6].**

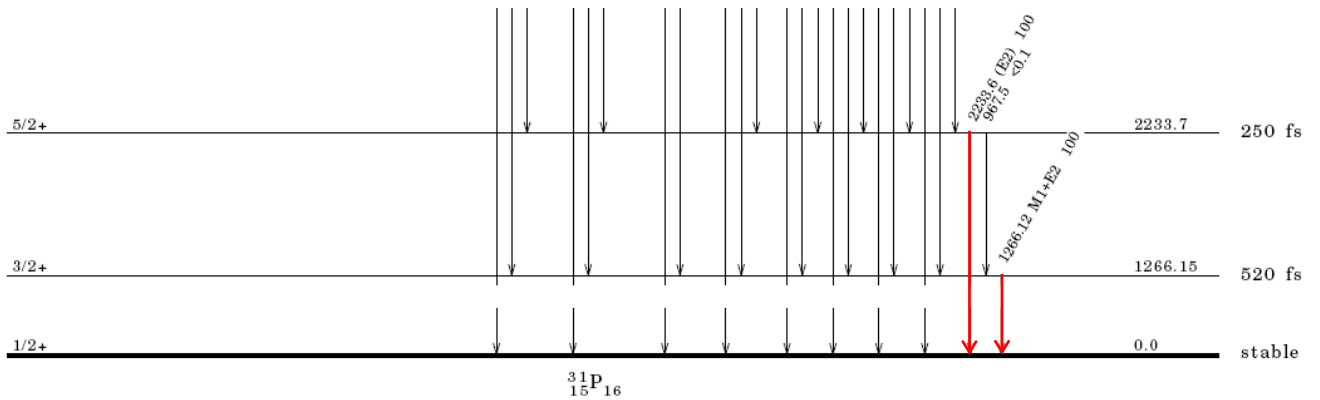
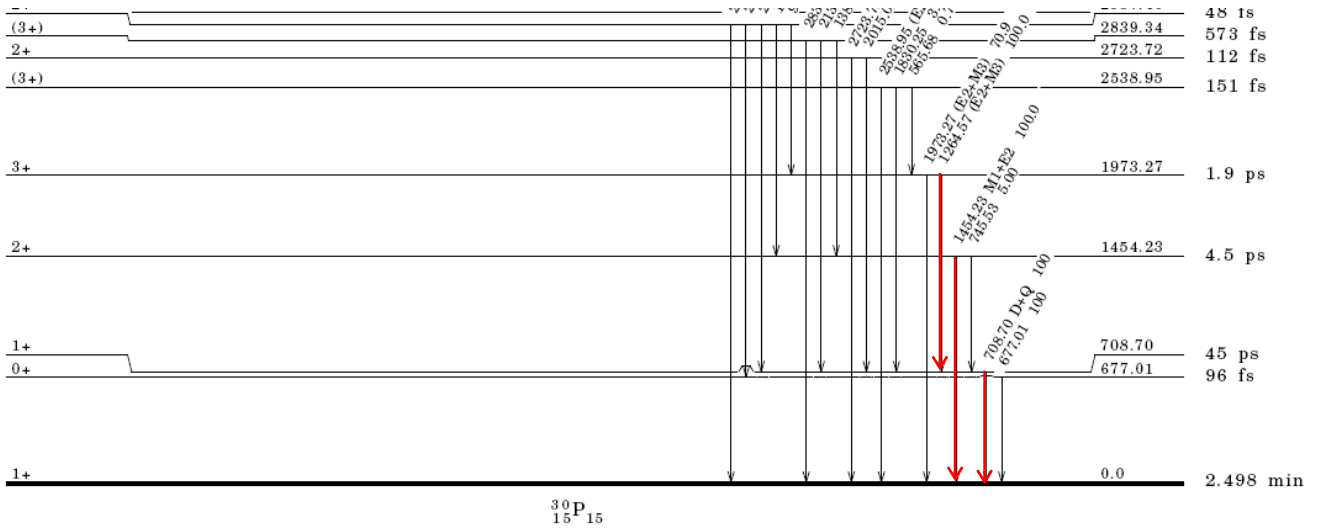
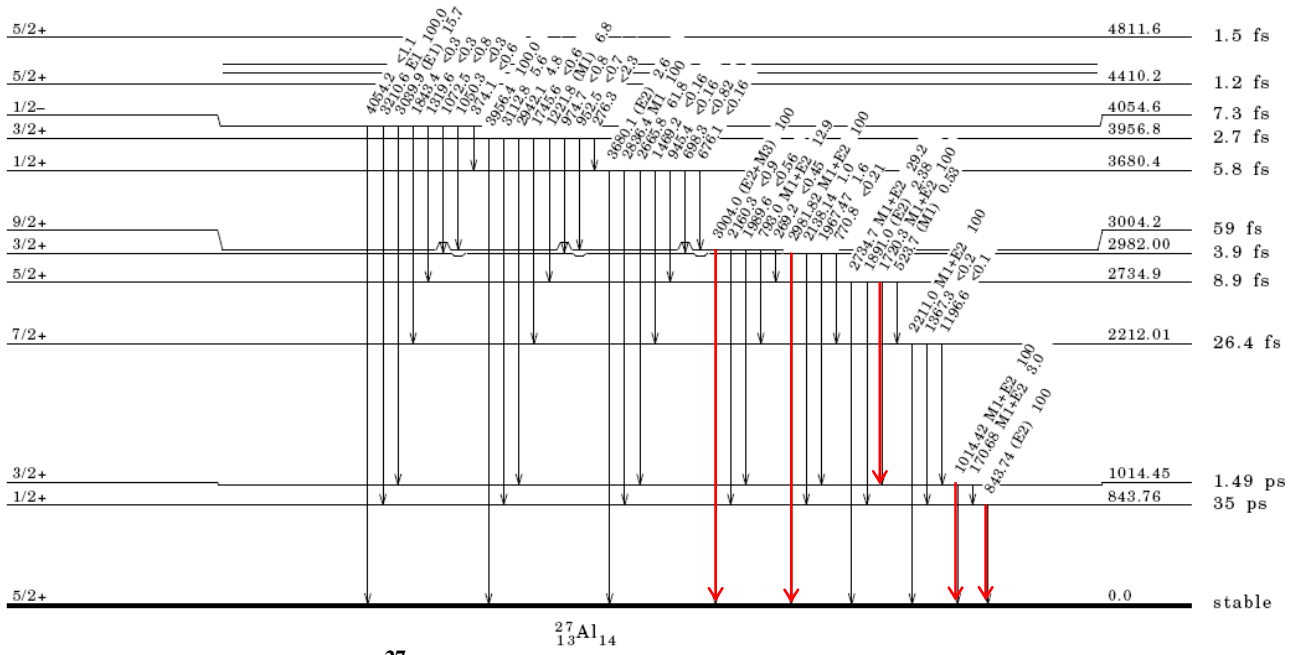
$E_{\gamma}$ [keV]	$I_{\gamma}$ [%]
311.9	38.5
300.129	6.63
340.476	4.45
415.764	1.73
398.492	1.391
375.404	0.679

**Table 7: The observed peaks, their possible origin, net peak areas and count rates.**

peak structure	$E_\gamma$ [keV]	isotope	gain 50		gain 10	
			area	cnt/s	area	cnt/s
narrow, single	708.7	30P	70236.9	1.24		
narrow, single	843.74	27Al	12005.3	0.21		
narrow	955.8	?	2972	0.05		
narrow	962.1	?	6043	0.11		
narrow, single	1014.42	27Al	9685.8	0.17		
broad, multiple	1263.13	30Si	83659	1.47	123780	1.52
	1264.57	30P				
	1266.12	31P				
	1271.9	30Si				
broad, single	1311.8	30Si	10549	0.19	14777	0.18
narrow, single	1454.23	30P	22967	0.40	38889	0.48
broad, single	1534.12	30Si	14595	0.26	22068	0.27
narrow, single	1552.36	30Si	5851	0.10	9526	0.12
broad, multiple	1720.3	27Al	37769	0.66	59675	0.73
	1732.7	30Si				
broad, overlaps with Compton	1989.02	30Si				
broad, maybe multiple	2233.6	31P	351738	6.19	509136	6.25
	2235.23	30Si				
broad, single	2595.39	30Si	29897	0.53	46330	0.57
broad, multiple	2981.82	27Al			18736	0.23
	3004	27Al				
broad, multiple	3039	30Si			32249	0.40
	3043.2	30Si				
broad, single	3252	30Si			8153	0.10
broad, single	3498.33	30Si			61709	0.76
weak	3714.9	30Si				
broad, single	3769.22	30Si			9939	0.12
broad	4300	?			3584	0.04
broad, single	4810	30Si			8147	0.10
narrow	7124	?			144	0.002
narrow	7303	?			106	0.001
narrow	7400	?			279	0.003
narrow	7634	?			123	0.002
narrow	7913	?			309	0.004







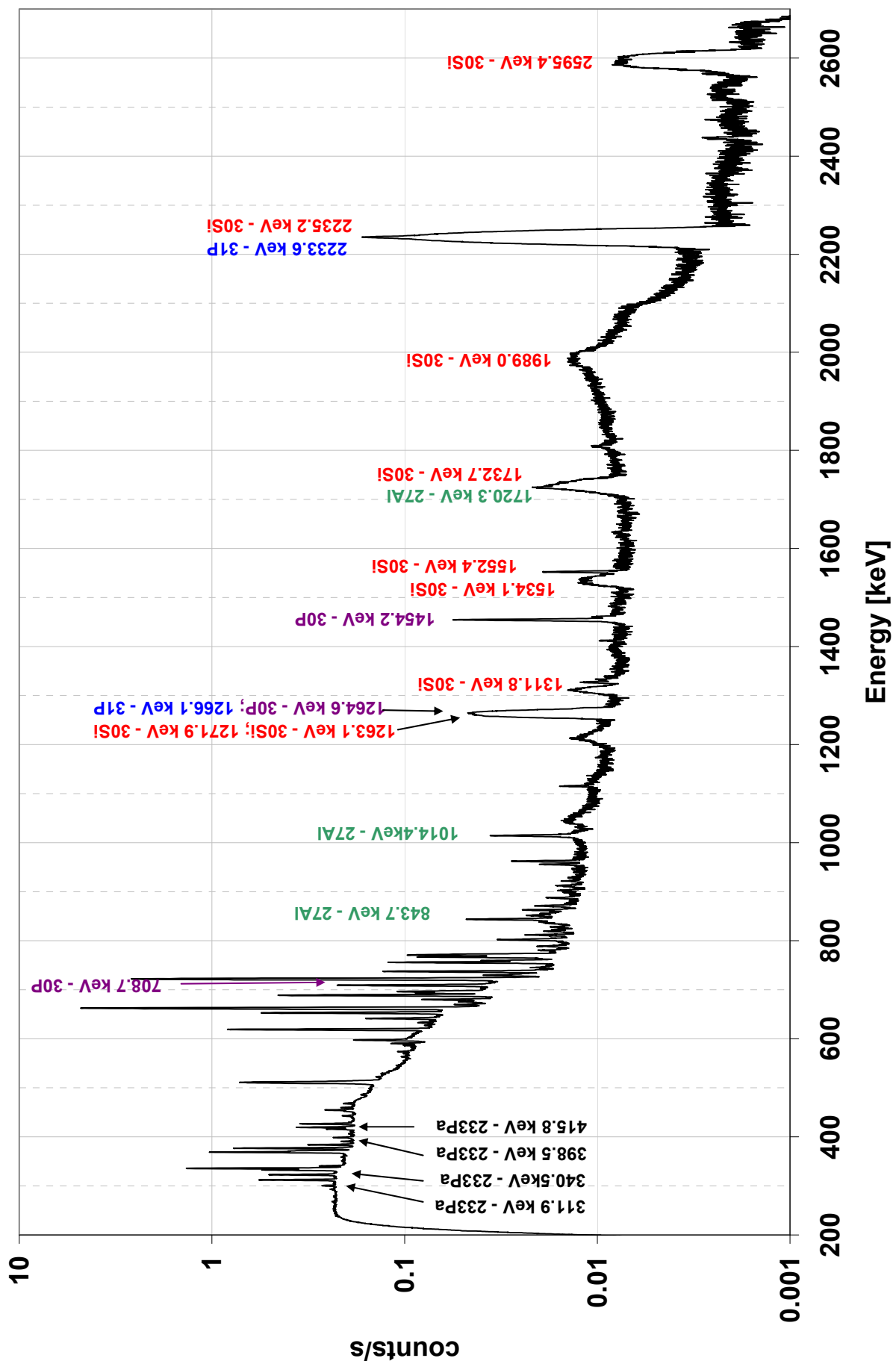


Figure 6: The whole americium spectrum measured with gain = 50.

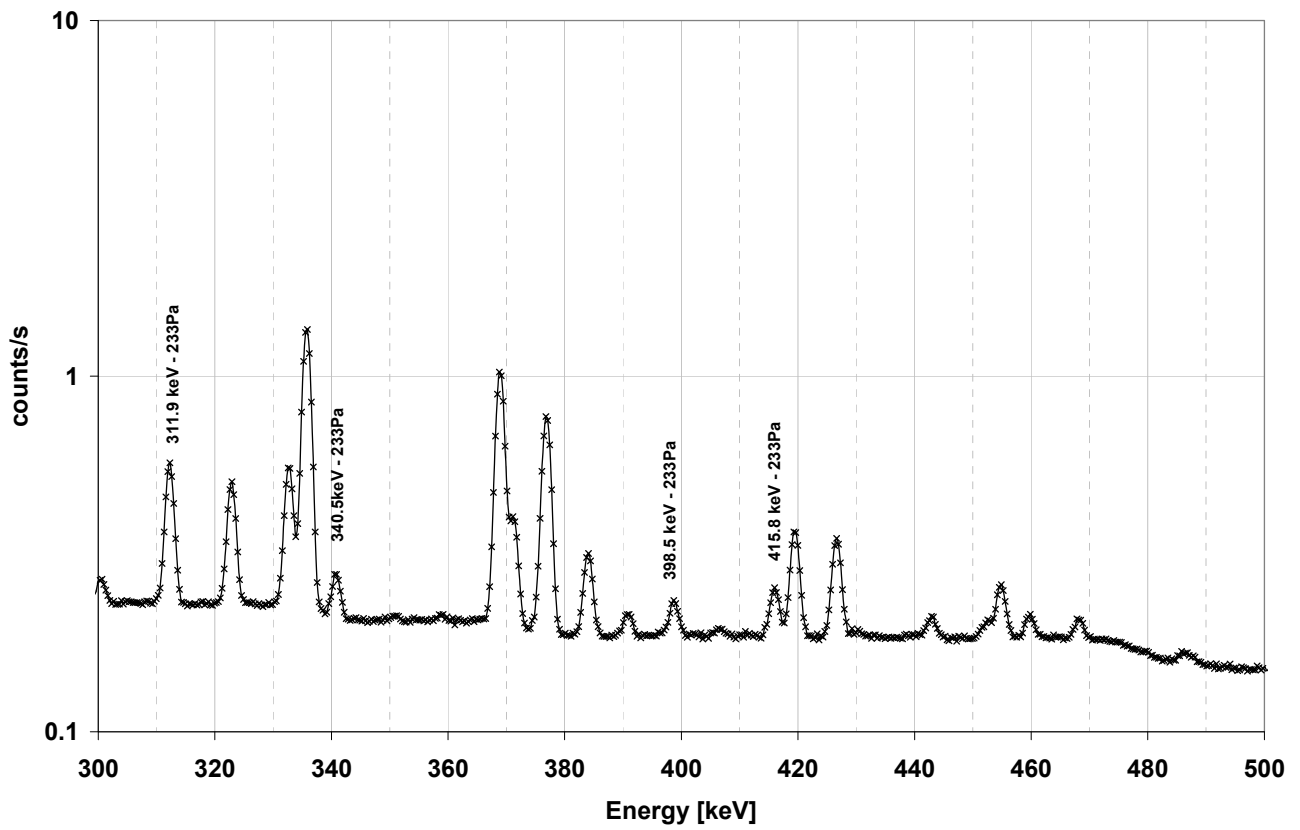


Figure 7: A detail (300-500 keV) of the americium spectrum measured with gain = 50.

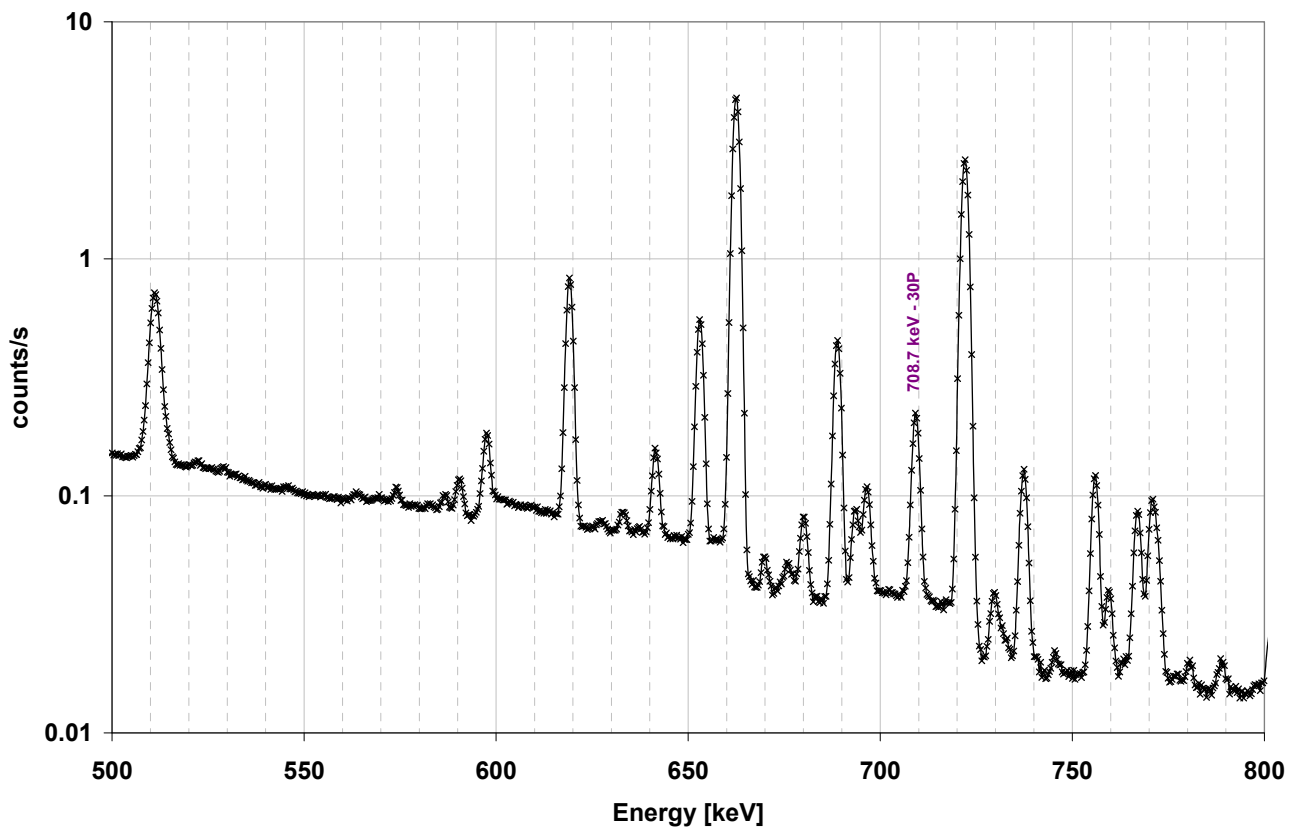


Figure 8: A detail (500-800 keV) of the americium spectrum measured with gain = 50.

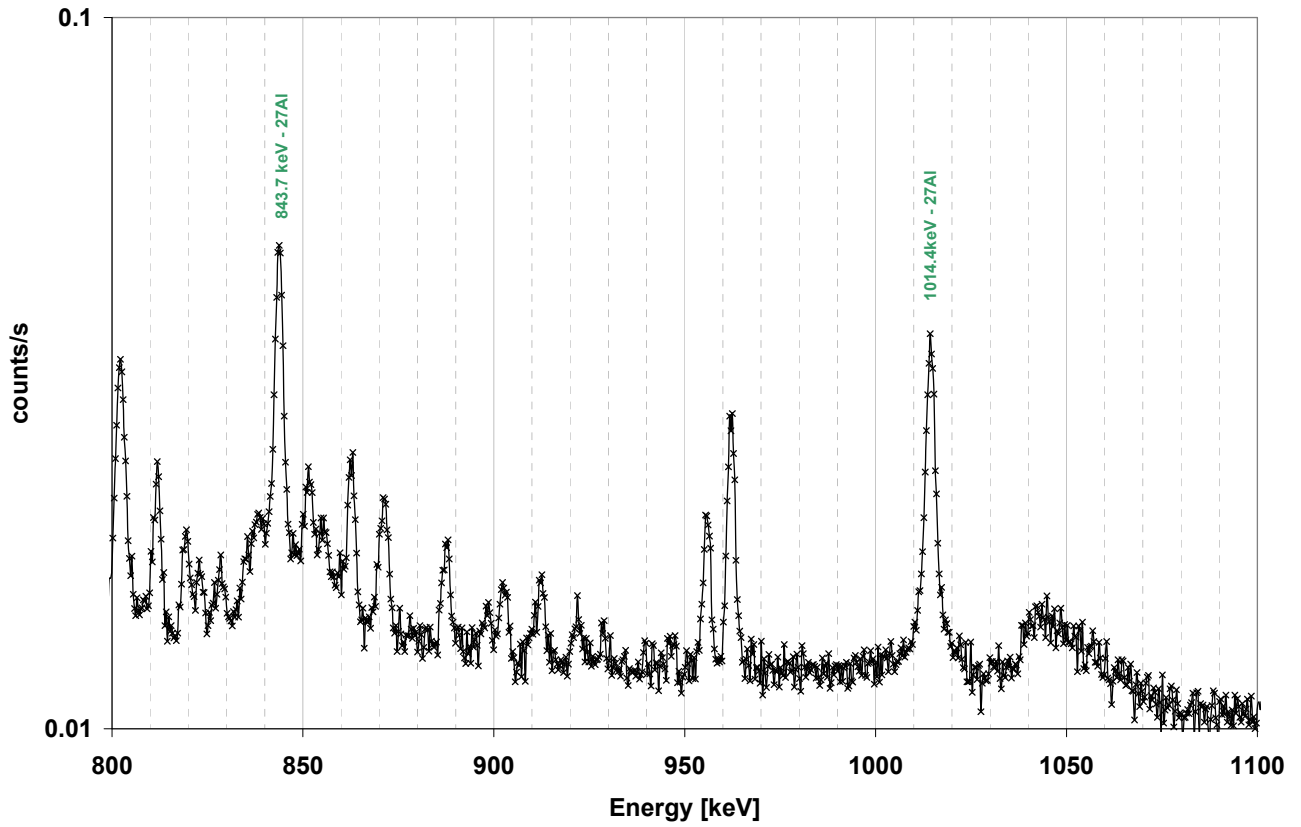


Figure 9: A detail (800-1100 keV) of the americium spectrum measured with gain = 50.

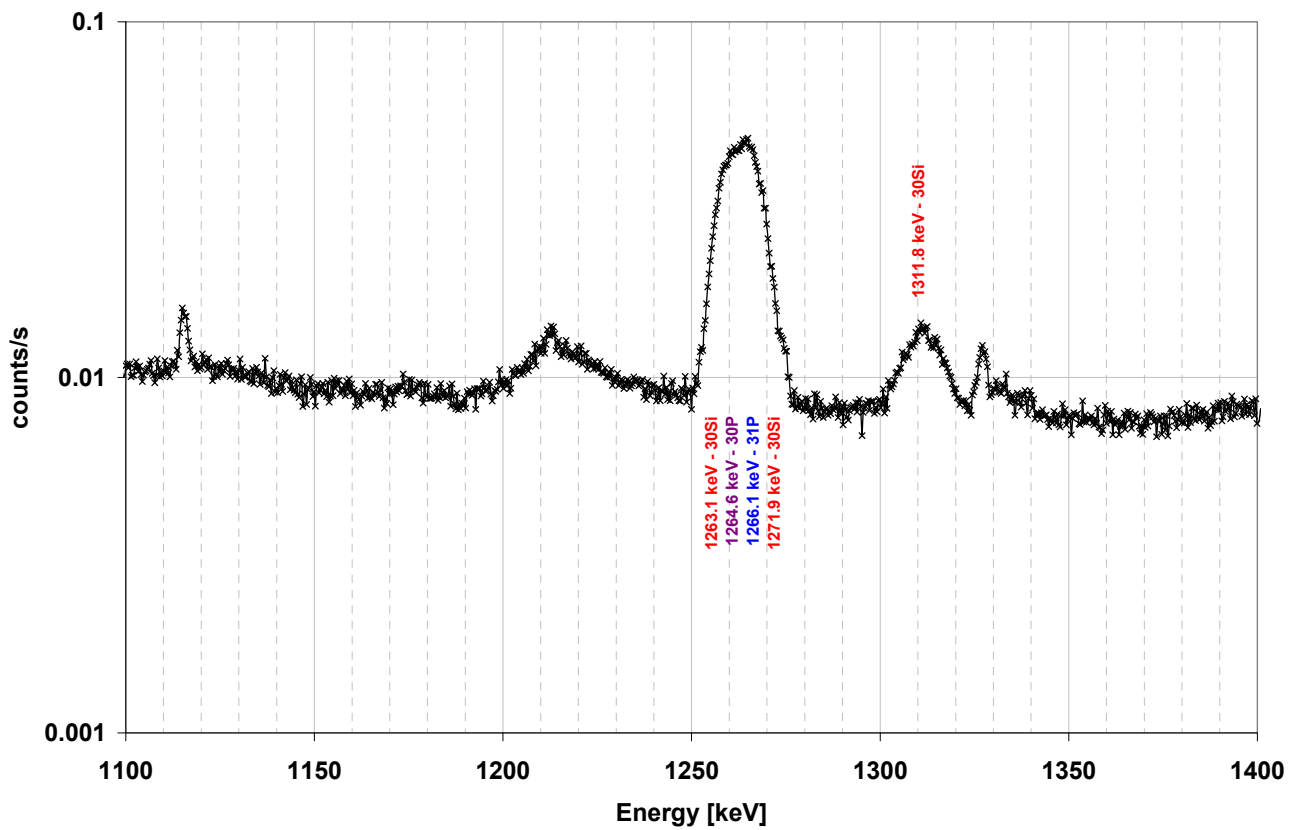


Figure 10: A detail (1100-1400 keV) of the americium spectrum measured with gain = 50.

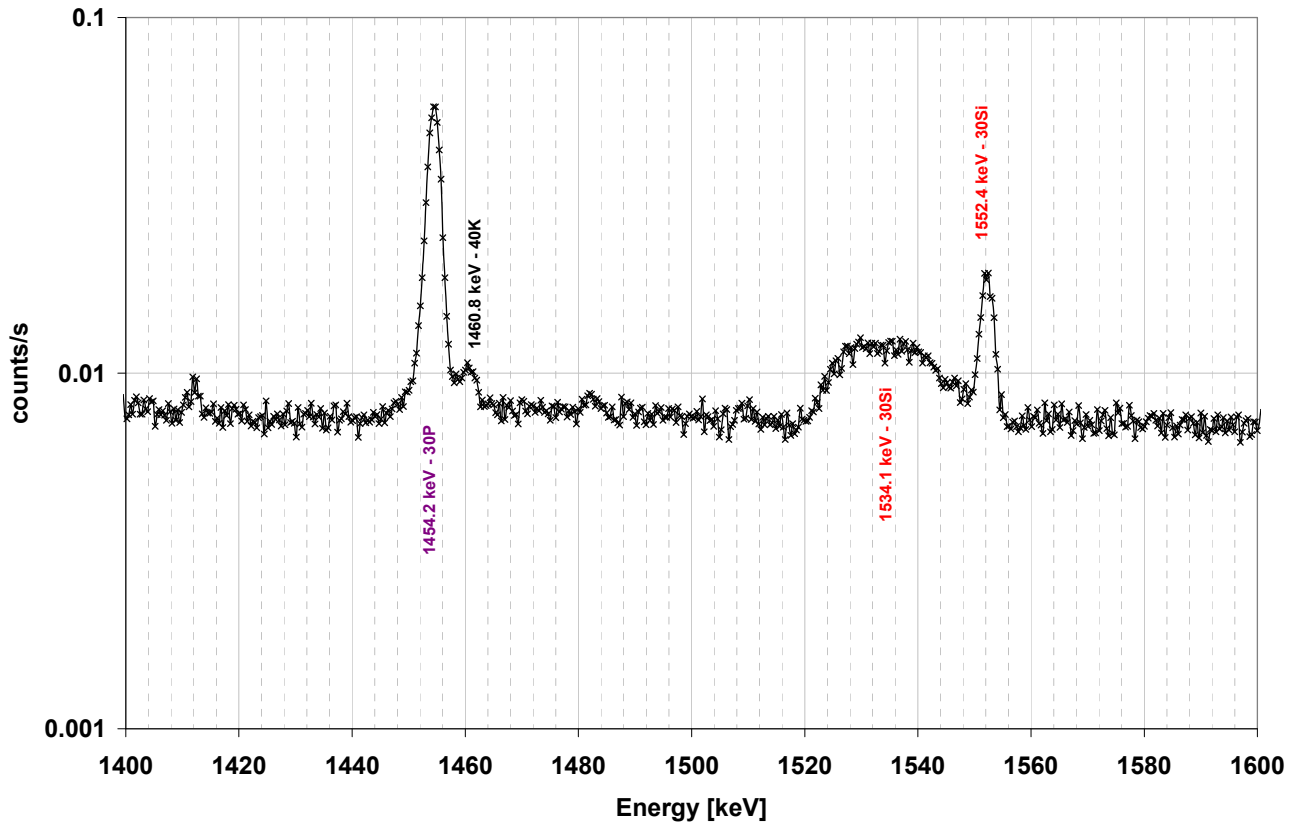


Figure 11: A detail (1400-1600 keV) of the americium spectrum measured with gain = 50. The 1460.8 keV line is clearly separated from 1454.2 keV.

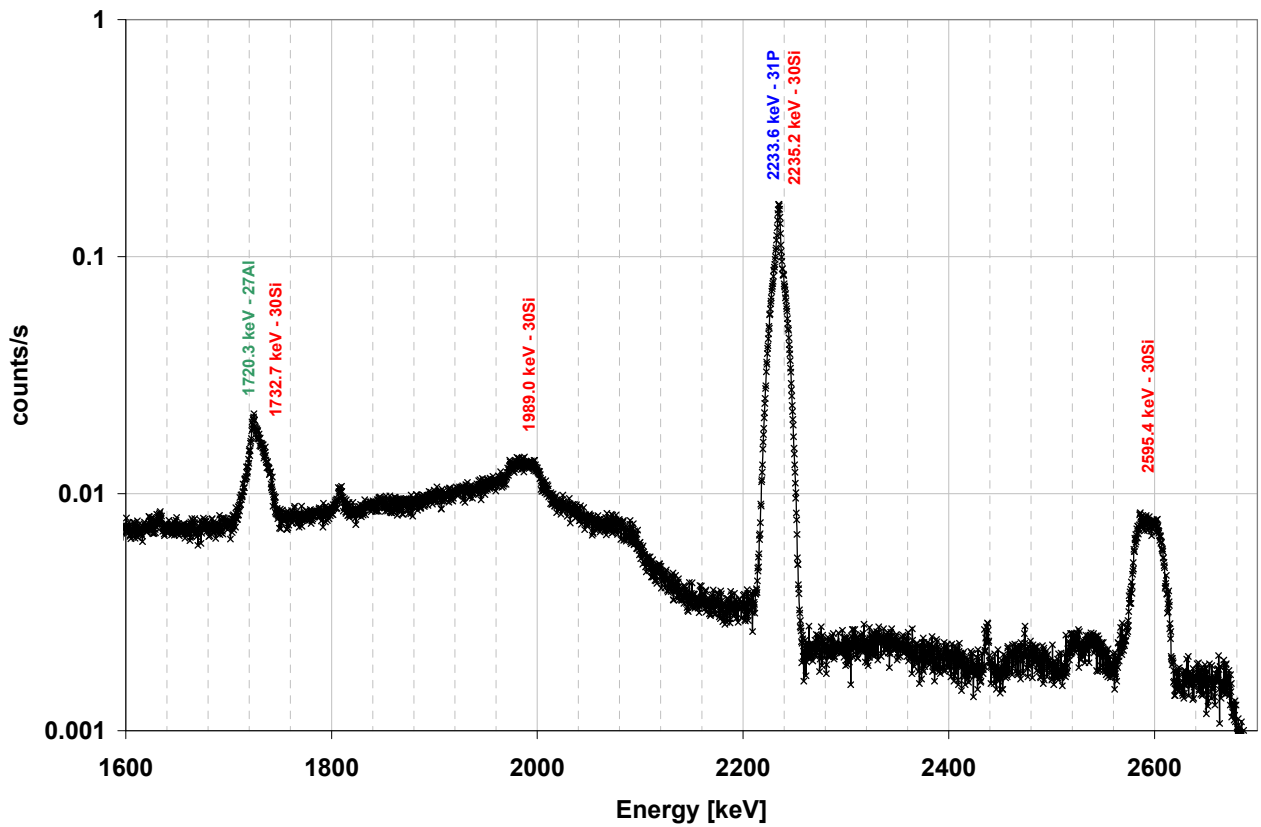


Figure 12: A detail (1600-2700 keV) of the americium spectrum measured with gain = 50.

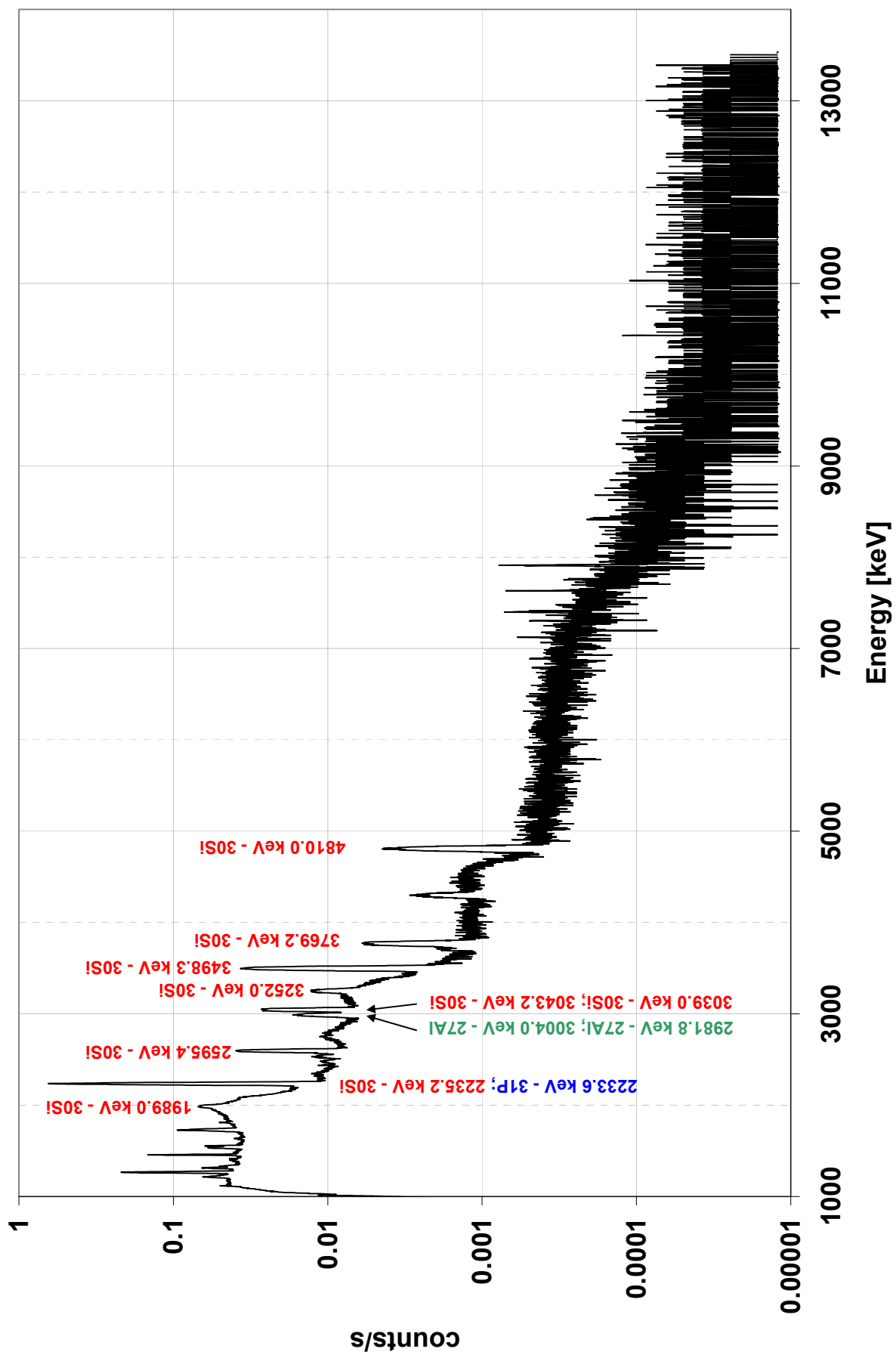


Figure 13: The whole americium spectrum measured with gain = 10.

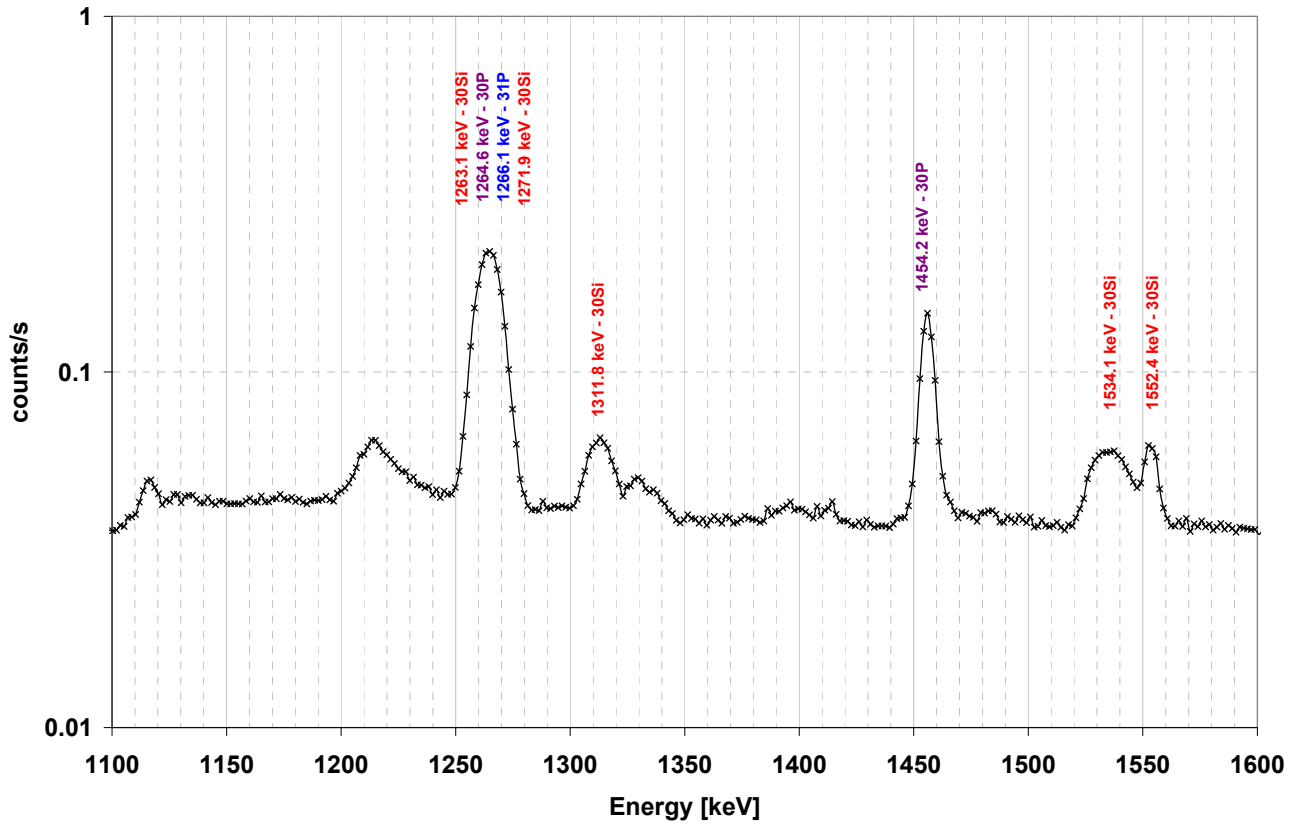


Figure 14: A detail (1100-1600 keV) of the americium spectrum measured with gain = 10.

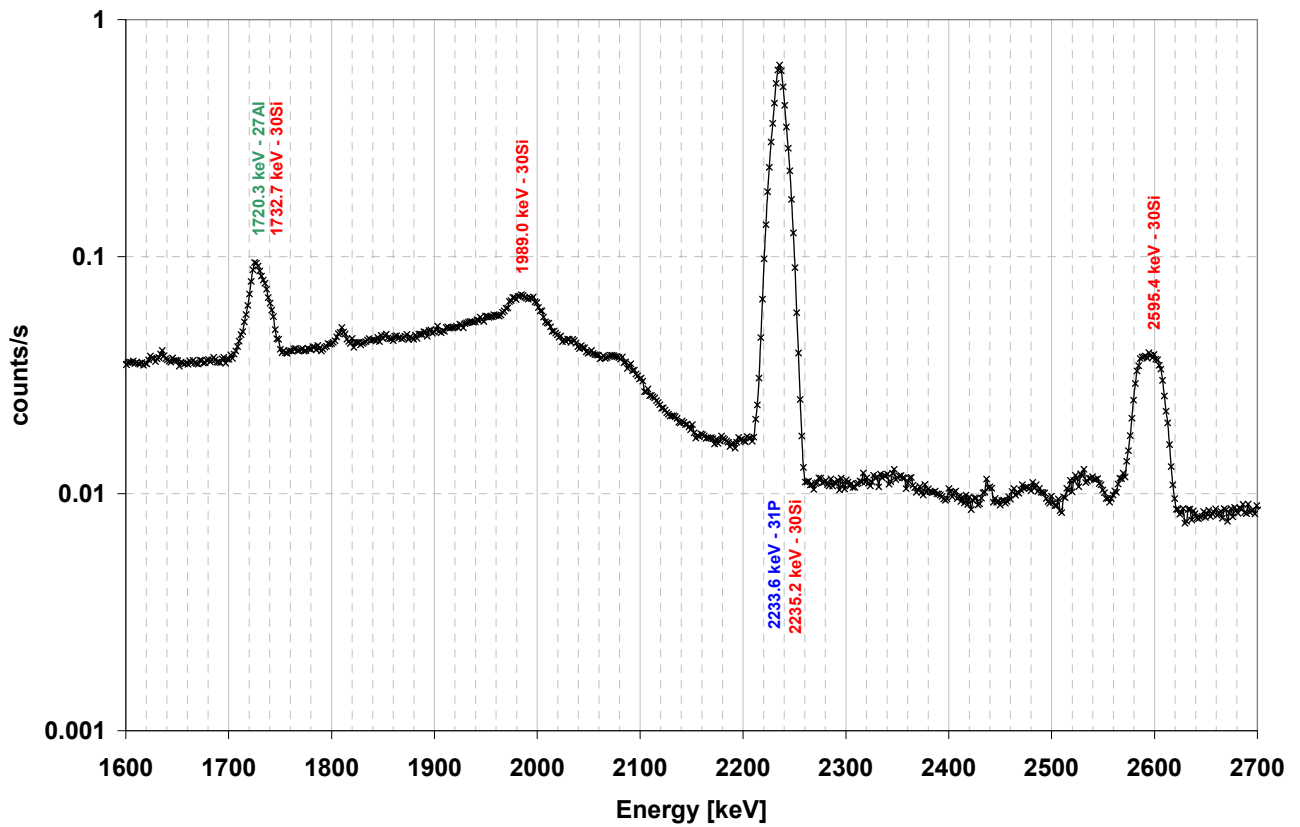


Figure 15: A detail (1600-2700 keV) of the americium spectrum measured with gain = 10.



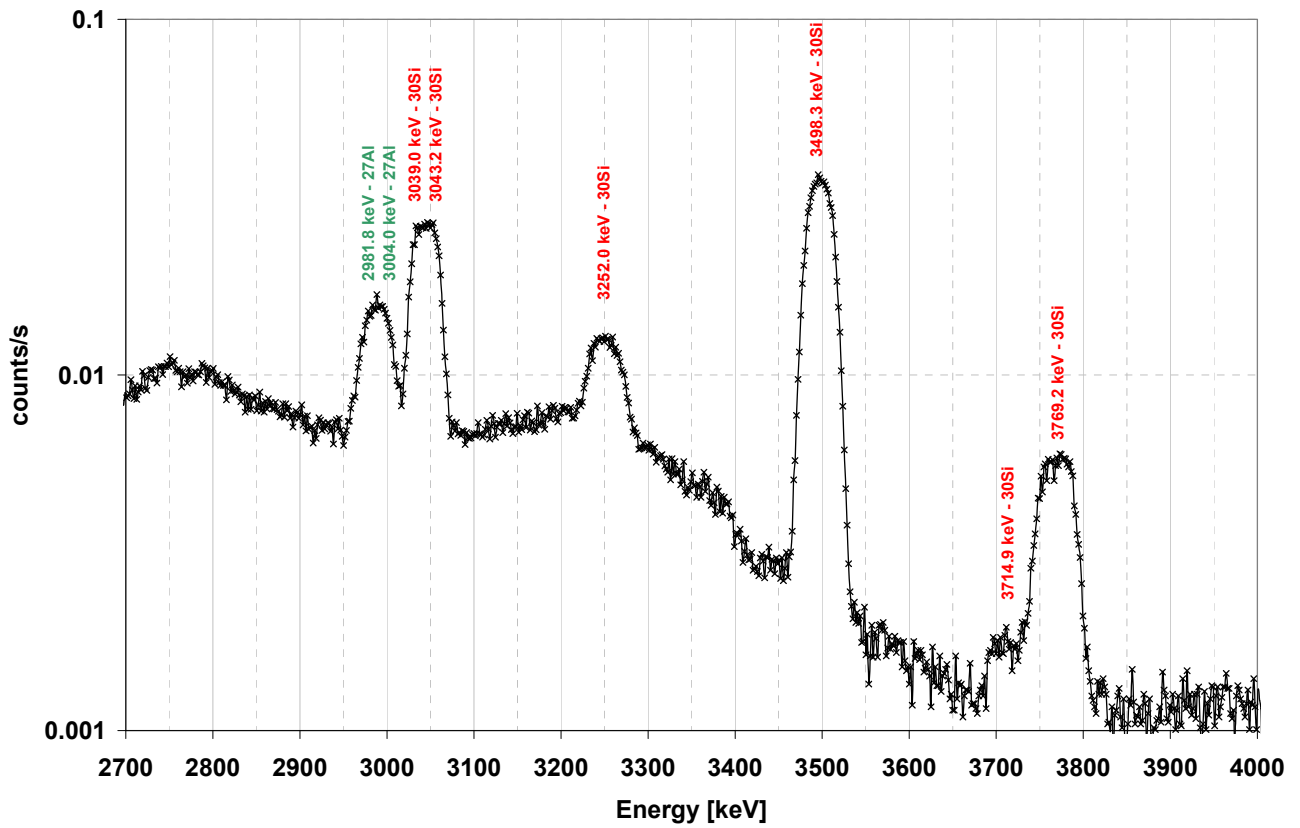


Figure 16: A detail (2700-4000 keV) of the americium spectrum measured with gain = 10.

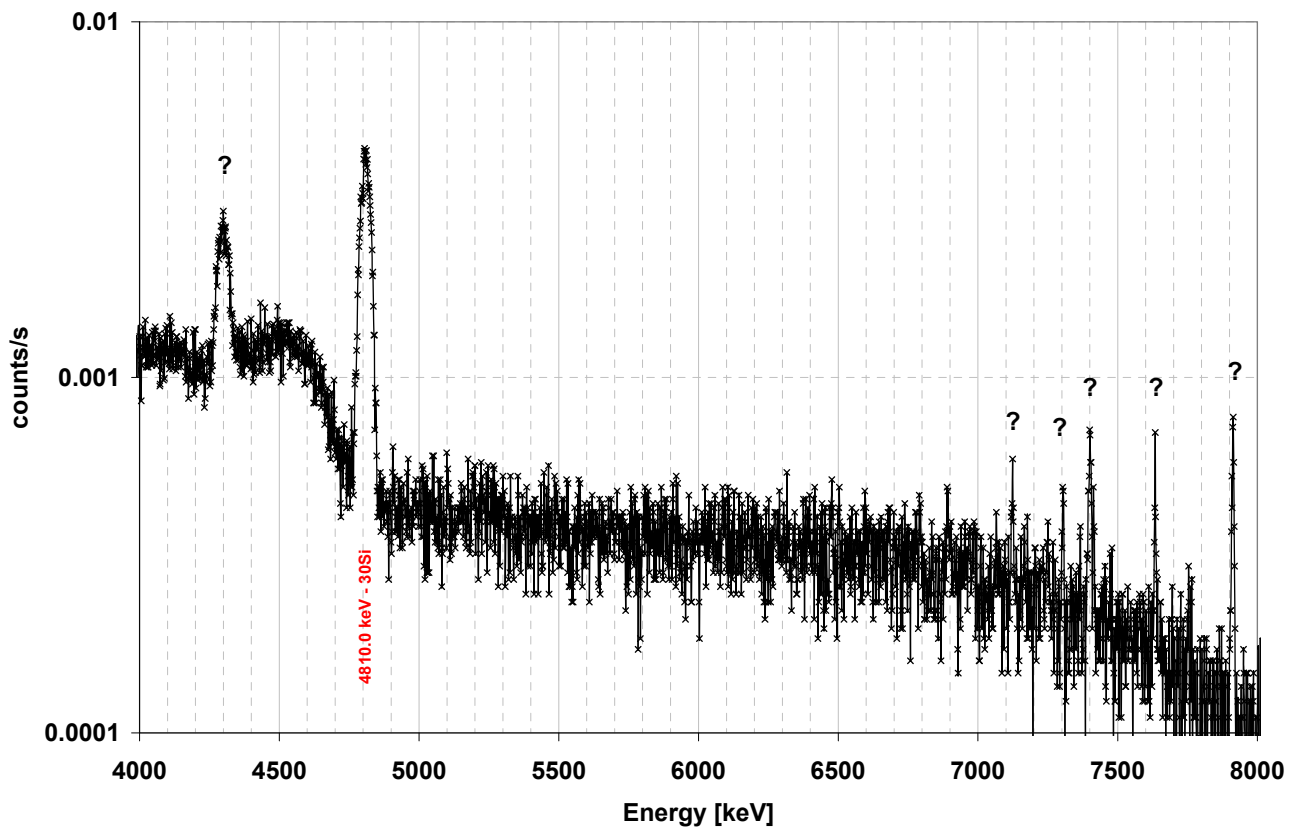
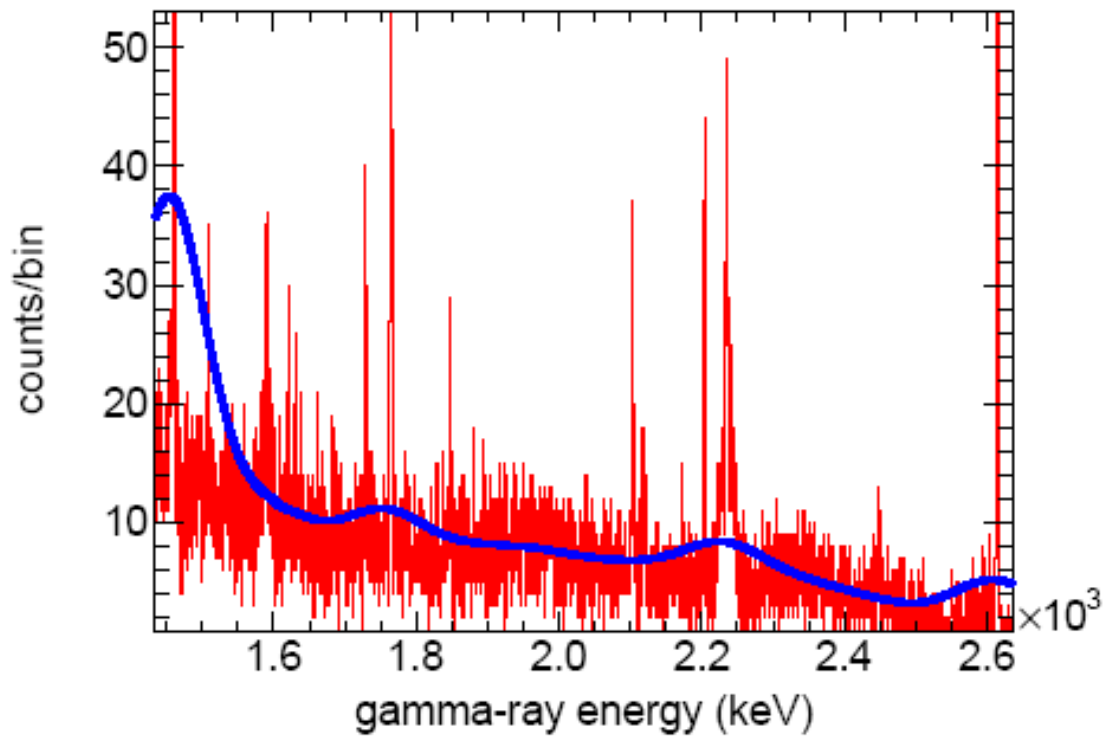


Figure 17: A detail (4000-8000 keV) of the americium spectrum measured with gain = 10. The unidentified peaks are shown.



**Figure 18: The americium spectrum measured in CERN in December 2010.**

## References

- [1] C. Sage, *High resolution measurements of the  $^{241}\text{Am}(n,2n)$  reaction cross section*, Physical review C 81, 064604 (2010).
- [2] C. Nästrén et al., *Fabrication of Am samples for neutron cross section measurements at JRC-IRMM Geel*, technical note JRC-ITU-TN-2006/34.
- [3] M. J. Martin, Nuclear Data Sheets 106, 89 (2005).
- [4] P.M. Endt, J. Blachot, R.B. Firestone, J. Zipkin, Nuclear Physics A633, 1 (1998)
- [5] M. Shamsuzzoha Basunia, Nuclear Data Sheets 111, 2331 (2010)
- [6] Balraj Singh and Jagdish K. Tuli, Nuclear Data Sheets 105, 109 (2005)

European Commission

**EUR 24818 EN – Joint Research Centre – Institute for Reference Materials and Measurements**

Title: Gamma-rays from a  $^{241}\text{AmO}_2$  source in an  $\text{Al}_2\text{O}_3$  matrix

Authors: Antonín Krása and Arjan Plompen

Luxembourg: Publications Office of the European Union

2011 – 11 pp. – 21.0 x 29.7 cm

EUR – Scientific and Technical Research series – ISSN 1831-9424

ISBN 978-92-79-20245-2

doi:10.2787/43859

**Abstract**

High energy gamma-rays emitted by a 40 mg  $^{241}\text{Am}$  source in the form of  $\text{AmO}_2$  dispersed in a  $\text{Al}_2\text{O}_3$  matrix were measured with a high purity germanium detector. The origin of the most intense gamma-rays was identified to the extent that these do not originate from the decay of  $^{241}\text{Am}$ . These gammas are due either to the decay of  $^{233}\text{Pa}$  (for energies below 400 keV), a daughter of the main actinide impurity ( $^{237}\text{Np}$ ) or to alpha-induced reactions on aluminium (for energies from 844 to 4810 keV). For the latter, the most important is the  $^{27}\text{Al}(\alpha, p)^{30}\text{Si}$  reaction, but one also observes gammas from the  $^{27}\text{Al}(\alpha, \gamma)^{27}\text{Al}$  and  $^{27}\text{Al}(\alpha, n)^{30}\text{P}$  reactions. There is no evidence for alpha-induced reactions on the isotopes of oxygen.

**How to obtain EU publications**

Our priced publications are available from EU Bookshop (<http://bookshop.europa.eu>), where you can place an order with the sales agent of your choice.

The Publications Office has a worldwide network of sales agents. You can obtain their contact details by sending a fax to (352) 29 29-42758.

The mission of the JRC is to provide customer-driven scientific and technical support for the conception, development, implementation and monitoring of EU policies. As a service of the European Commission, the JRC functions as a reference centre of science and technology for the Union. Close to the policy-making process, it serves the common interest of the Member States, while being independent of special interests, whether private or national.

